Environmental Pollution 293 (2022) 118432

Contents lists available at ScienceDirect

Environmental Pollution

journal homepage: www.elsevier.com/locate/envpol

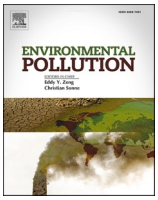

Source attribution and quantification of atmospheric nickel concentrations in an industrial area in the United Kingdom (UK)☆

Anna Font [a,*], Anja H. Tremper [a], Max Priestman [a], Frank J. Kelly [a], Francesco Canonaco [b], André S.H. Prévôt [b], David C. Green [a]

[a] MRC Centre for Environment and Health, Environmental Research Group, Imperial College London, 86 Wood Lane, London, W12 0BZ, UK
[b] Paul Scherrer Institute, Laboratory of Atmospheric Chemistry, Villigen PSI, 5232, Switzerland

ARTICLE INFO

Keywords:
Nickel
Stainless-steel production
Nickel refinery
Source apportionment
Positive matrix factorization
Cluster analysis

ABSTRACT

Pontardawe in South Wales, United Kingdom (UK), consistently has the highest concentrations of nickel (Ni) in PM_{10} in the UK and repeatedly breaches the 20 ng m^{-3} annual mean EU target value. Several local industries use Ni in their processes. To assist policy makers and regulators in quantifying the relative Ni contributions of these industries and developing appropriate emission reduction approaches, the hourly concentrations of 23 elements were measured using X-ray fluorescence alongside meteorological variables and black carbon during a four-week campaign in November–December 2015. Concentrations of Ni ranged between 0 and 2480 ng m^{-3} as hourly means. Positive Matrix Factorization (PMF) was used to identify sources contributing to measured elements. Cluster analysis of bivariate polar plots of those factors containing Ni in their profile was further used to quantify the industrial processes contributing to ambient PM_{10} concentrations. Two sources were identified to contribute to Ni concentrations, stainless-steel (which contributed to 10% of the Ni burden) and the Ni refinery (contributing 90%). From the stainless-steel process, melting activities were responsible for 66% of the stainless-steel factor contribution.

1. Introduction

Nickel (Ni) and other heavy metals such as arsenic (As), cadmium (Cd) and chromium (Cr) are characterized as human carcinogens (NIEHS, 2016). Epidemiological studies have found associations between adverse health outcomes and Ni exposure, such as respiratory hospital admissions (Bell et al., 2014); cardiovascular and respiratory mortality and all-cause mortality (Zhang et al., 2009); and low birthweight (Bell et al., 2010). Ni is an important source for cellular oxidant generation and may be responsible, in part, for health effects associated with particle air pollution (MacIejczyk et al., 2010). With the aim of minimizing harmful effects on human health the 4th European Daughter Directive 2004/107/EC set a Target Value (TV) for atmospheric Ni concentrations in PM_{10} to be less than 20 ng m^{-3} as annual mean (European Parliament and Council of the European Union, 2004). Member States are required to identify zones and agglomerations where exceedances of the TV occur and report a series of measures to reduce emissions. The first step to achieve this is to identify the sources and their contribution to ambient concentrations.

Ni is emitted to the atmosphere mainly arising from anthropogenic activities such as the combustion of coal, diesel and fossil oil; from metallurgical, iron and steel manufacturing; mining and refining; as well as from the incineration of waste and sewage (Cempel and Nikel, 2006; Nriagu and Pacyna, 1988; Pacyna et al., 1984). Ni and vanadium (V) are co-emitted in fuel oil combustion for residential and commercial heating (Peltier et al., 2009); shipping emissions (Cesari et al., 2014; Kfoury et al., 2016; Pandolfi et al., 2011; Viana et al., 2014); and oil refineries (Sánchez de la Campa et al., 2011). Metallurgical activities emit Ni alongside Cr, manganese (Mn) and copper (Cu) (Alastuey et al., 2016; Querol et al., 2007). Iron and steel foundries, including stainless-steel castings are also a source of atmospheric Ni alongside lead (Pb), Mn, Cd and Cr (US EPA, 2016). Ni is also emitted by incinerators of municipal waste alongside As, Cd, Cr, Cu, Pb, Mn and V; however, non-distinctive emission profiles containing Ni were identified in UK municipal waste incinerators (Font et al., 2015). In ambient studies Ni, Cr and Mn profiles were associated with intermittent industrial plumes

☆ This paper has been recommended for acceptance by Pavlos Kassomenos.

* Corresponding author.
E-mail address: anna.font@imperial.ac.uk (A. Font).

https://doi.org/10.1016/j.envpol.2021.118432
Received 15 October 2020; Received in revised form 18 October 2021; Accepted 28 October 2021
Available online 3 November 2021

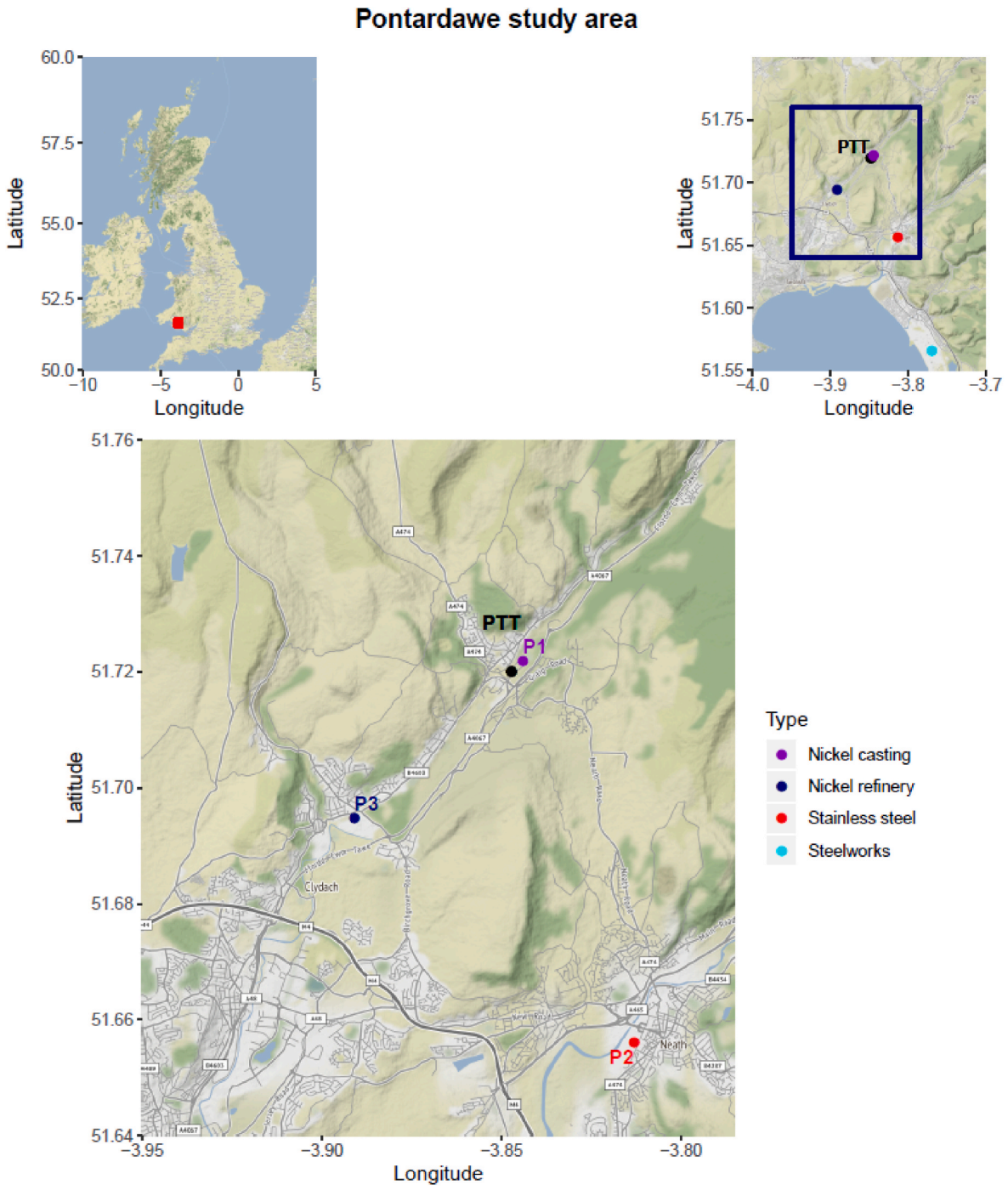

Fig. 1. Map of the study area. The monitoring site belonging to the Defra Heavy Metals Network is indicated in black PTT (Pontardawe Tawe Terrace). Industrial sources are indicated in coloured dots (P1, P2, P3).

(Rai et al., 2020).

Concentrations of Ni and other heavy metals in airborne particulate matter with diameter <10 μm (PM_{10}) are routinely measured in the United Kingdom (UK) as part of the UK Heavy Metals network. PM_{10} was sampled for seven days and subsequently analysed by inductively coupled plasma mass spectrometry (Goddard et al., 2015). In 2014, the Pontardawe Tawe Terrace breeched the TV with an annual mean concentration of 43 ng m^{-3} (Goddard et al., 2015) and despite the annual concentration in 2015 being reduced to 27.8 ng m^{-3}, this was still 139% the TV (Goddard et al., 2016). The site is in an industrialised area where Ni is used in different processes and therefore identification and quantification of the sources (industrial and non-industrial) contributing to the breech of the TV is needed. Weekly measurements are valuable in calculating annual concentrations and monitor long-term changes over time. However, the low sampling frequency makes it difficult to apportion which sources contribute to ambient concentrations.

Positive Matrix Factorization (PMF) is a mathematical receptor model widely used in the atmospheric community to identify and quantify the contribution of sources to ambient concentrations in urban and rural environments (e.g. Mooibroek et al., 2011) but also in industrial areas (Alleman et al., 2010; Bozlaker et al., 2013; Kara et al., 2015; Kfoury et al., 2016). PMF receptor modelling is used when the number of sources is unknown and thus it can be used to find both the profiles (chemical composition) and their contributions based on internal

correlations of elements and tracers measured in a set of samples (Paatero and Tapper, 1994).

The aim of this study was to identify and quantify the emissions of nickel from the key sources in and around Pontardawe which led to breeches of the EU Air Quality Directive Target Value. A campaign measuring metals concentrations in PM_{10} at an hourly resolution was undertaken using the Mobile Atmospheric Research PLatform (MARPL) in Pontardawe (27 Nov - Dec 24, 2015) alongside the long-running UK Heavy Metals monitoring site (Defra). PMF was used to identify the sources and those industrial processes contributing to the ambient concentrations based on the chemical composition. Bivariate polar plots for the factor time series containing Ni in the chemical profile were built and cluster analysis applied to pinpoint and quantify the contribution of each industry to each source process.

2. METHODS

2.1. Study areas

The Pontardawe Tawe Terrace monitoring site (PTT; 51°43′12″N, 3°50′50″W) in South Wales is located in a narrow river valley with several industries (Fig. 1A). Located 300 m north-east of PTT a nickel alloy production facility (P1 in Fig. 1) manufactures surfacing and brazing products, castings and engineered components, using 30–40,000 tons of Ni per annum. Emissions from P1 are expected to be released through the stack arising from melting activities in the furnaces; and fugitive from both non-melting activities (such as mould making and preparation, fettling and cut off, charge formulation, sieving grading and packaging); and also resuspension of material). Melting activities took place overnight from 10 pm to 6 am from Sundays to Thursdays. Non-melting activities took place on weekdays between 6 am and 10 pm At 7.2 km south-east of PPT an industrial site develops and produces advanced stainless-steel and special alloys using ~190 tonnes of Ni per annum. A nickel refinery is located 5 km south-west of PTT producing ~40,000 tonnes of nickel pellets and powder each year. The main points of emissions are the refinery stack (93 m height) and the effluent plant dryers from the Kiln plant (Martin et al., 2019). In 2015, a total of 146 kg of Ni was reported to be emitted to the atmosphere (E-PRTR, 2017).

2.2. Ambient measurements

Hourly concentrations of arsenic (As), barium (Ba), calcium (Ca), cerium (Ce), chromium (Cr), chlorine (Cl), copper (Cu), iron (Fe), potassium (K), manganese (Mn), nickel (Ni), lead (Pb), sulphur (S), antimony (Sb), selenium (Se), silicon (Si), strontium (Sr), titanium (Ti), vanadium (V) and zinc (Zn) in PM_{10} were measured using the Cooper Environmental Services Xact™ 625 automated multi-metals monitor at PTT from 27 November to December 24, 2015. The instrument is based on reel-to-reel filter tape sampling followed by non-destructive X-ray fluorescence (XRF) analysis. Daily automated quality assurance checks were performed every night at midnight with this hour missing for ambient measurements. Quality assurance and quality control of measurements included internal (palladium) and external standards checks (for all analysed metals); field blanks using a HEPA filter as well as tape blanks before and after each tape change for baseline; energy calibration; metals upscales (for Cd, Cr, and Pb) for instrument stability; and flow calibration.

The Limit of Detection (LOD) for each element was calculated from HEPA filter blank tests at the beginning and at the end of the campaign, estimated as three times the standard deviation. All hourly concentrations that were zero or below were replaced by 0.5*LOD for data reporting. A detailed evaluation of the precision and accuracy of the instrument and as well an inter-comparison of the XACT measurements against other analytical methods can be found in Furger et al. (2017) and Tremper et al. (2017). A further inter-comparison between the XACT measurements and the weekly samples was done. Weekly samples were performed on filters analysed by the ICP-MS methodology as described in Goddard et al. (2015). The comparison showed slopes ranging from 0.96 (Zn) and 1.24 (Pb) with a slope of 1.10 for Ni; and the correlation coefficient (R^2) ranged between 0.74 (Zn) and 0.99 (Ni and V).

The Magee Scientific Aethalometers (AE-22) was deployed and measured the aerosol light absorption coefficient collected on a quartz filter at two wavelengths (370 and 880 nm). The instrument calculates the absorption coefficient of the sample by measuring the attenuation of the light passing through the sample relative to a clean piece of filter. The change in the attenuation is converted to black carbon (BC) using a mass extinction coefficient of 16.6 $m^2\ g^{-1}$ chosen by the manufacturer to give a good match to elemental carbon. In practice the mass extinction coefficient varies with factors such as particle size, sample composition and quantity of material already on the filter. The effect of this nonlinearity due to filter loading was corrected using the model developed by Virkkula et al. (2015). The aethalometer was equipped with a $PM_{2.5}$ inlet and measured at a 15-min resolution. The multi-wave absorption measurements were used to apportion BC to two main fractions: fossil fuel (BC_{ff}) and wood burning (BC_{wb}) following the aethalometer model first presented by Sandradewi et al. (2008). Absorption coefficients of 2.1 for pure wood burning; and 0.96 for traffic were used in accordance with values reported in Fuller et al. (2014).

Wind speed, wind direction and temperature were measured at 10 m using a Met One AIO2 weather sensor installed at MARPL.

2.3. Source apportionment

The Source Finder SoFi Pro toolkit (Canonaco et al., 2013) (Datalystica Ltd., Villigen, Switzerland) for Igor Pro (WaveMetrics, Inc., Portland, Oregon, USA) was used to apportion the different sources of elements and metals in PTT. SoFi Pro uses the Multilinear engine solver (Paatero, 1999) (ME2) to perform Positive Matrix Factorization (Paatero and Tapper, 1994). A description of the model can be found elsewhere, and a summary is presented in the Supplementary Information (Section 3.1).

The hourly concentrations of all elements measured with the XACT instrument and their uncertainties were used to run the model (input matrix). The uncertainties were propagated accounting for the uncertainty of the flow ($3/\sqrt{3}\%$); the uncertainty from the calibration standard (5%) (US-EPA, 1999); the long term stability, calculated from the standard deviation of hourly internal Pd reference (2.9%); and an element-specific uncertainty associated with the spectral deconvolution calculated by the instrument software for each spectra. The data input for the PMF model was as reported by the instrument and corrected by the blank, without any modification or censoring of data below the LOD or equal or less than zero as recommended by Brown et al. (2015).

Variables were classified as good, weak or bad depending on their average signal–to–noise ratio (S/N) according to Paatero and Hopke (2003). Variables with $S/N < 0.2$ were classified as bad and removed from analysis (Ba, Cd, Ce, Mo, Sb, Se, Sr); and elements with $0.2 < S/N < 2$ were classified as weak. The uncertainty of weak species was weighted by factor of 10. The dimensions of the input matrix for PMF were 15 x 595 (species x observations).

Running unconstrained PMF showed the difficulties to separate the two Ni sources. To overcome this, a first PMF was run excluding those samples when Ni was present but didn't contain Cr (size input matrix: 15 (species) x 455 (observations)). This was done to exclude the Ni sources non-related with the stainless-steel production. A seven-factor solution was reported to be the best based on the Q/Q_{exp} (Supplementary Figure 3); Ni/Cr for the source containing Ni was 4.56 (Supplementary Figure 4), in agreement with the range of Ni to Cr ratios made available from P1 (4.35–21.03). The chemical composition for other factors (traffic, solid fuel combustion and dust) were also extracted from this run. A second run was undertaken reintroducing the excluded samples (those with Ni but without Cr) and constrained for four factors from the

Table 1
Average hourly concentrations (ng m^{-3}) of elements measured at Pontardawe Tawe Terrace (25 Nov – Dec 24, 2015); mean: arithmetic mean; mG: geometric mean; sd: standard deviation; min: minimum, Q1, Q2, Q3: quartile 25%, 50%, 75%; max: maximum; N: number of hourly observations.

	mean	mG	sd	min	Q1	Q2	Q3	max	N	N below LOD (percent)
As	0.409	0	1.13	0	0	0	0.356	12.1	603	0 (0)
Ba	1.39	1.13	1.72	0.006	1.06	1.06	1.06	22.2	603	535 (88.7)
Ca	185	124	228	0.97	75	145	225	4060	603	0 (0)
Cd	2.98	2.4	1.46	0.002	2.19	3.43	3.43	11.5	603	591 (98.0)
Ce	0.839	0.597	0.695	0.012	0.347	0.595	1.18	4.88	603	156 (25.9)
Cl	5090	3070	3960	19.5	1520	4660	7600	18400	603	1 (0.2)
Cr	1.54	0.19	5.71	0.004	0.0645	0.0645	0.472	84.8	603	321 (53.2)
Cu	3.76	1.82	5.13	0.015	0.802	2.23	4.33	53.3	603	196 (32.5)
Fe	218	98.2	357	2.1	41.6	97.1	220	3570	603	1 (0.2)
K	151	123	97	4.15	92.1	132	191	694	603	71 (11.8)
Mn	3.03	1.49	5.45	0.002	0.768	1.42	2.98	78.3	603	6 (1.0)
Mo	1.12	0.51	8.28	0.002	0.552	0.552	0.552	199	603	448 (74.3)
Ni	19.5	0.907	146	0	0.282	0.802	3.17	2480	603	246 (40.8)
Pb	3.63	1.09	9.01	0.001	0.278	0.984	3.78	124	603	245 (40.6)
Pt	0.29	0.181	1.02	0.001	0.193	0.193	0.193	20.8	603	568 (94.2)
S	517	395	350	4.94	247	443	721	1780	603	2 (0.3)
Sb	0.135	0	3.31	0	0	0	0	81.2	603	0 (0)
Se	0.231	0.139	0.459	0.001	0.105	0.128	0.284	10.1	603	214 (35.5)
Si	270	122	693	0.355	102	102	102	7300	603	551 (91.4)
Sr	2.47	1.54	2.17	0.001	0.819	1.87	3.49	13	603	145 (24.0)
Ti	8.28	1.79	22.4	0.004	0.528	1.45	4.61	169	603	92 (15.3)
V	1.09	0.415	1.76	0.002	0.176	0.251	1.05	11.3	603	217 (36.0)
Zn	7.08	2.49	13.2	0.013	0.828	2.81	8.51	147	603	50 (8.3)

first unconstrained run (stainless-steel, traffic, solid fuel combustion and dust). Factors were constrained with a low a-value (random a-value of 0–0.1). The 11-factor solution was the one separating the two Ni sources; and the bivariate polar plots showed that each source was pointing to the different industrial sources using Ni (Supplementary Figure 5).

A third PMF run was done to decide the optimal number of profiles. Five factors were constrained (stainless-steel, nickel refinery, traffic, solid fuel combustion and dust) with an exact a-value of 0.3. A range of solutions with varying number of factors (3–15) was examined. The selection of the solution with the optimal number of factors was based on the reduction of the Q/Q_{exp} ratio when adding an extra factor and also by the goodness of representation of the sum of species. The 8-factor solution was then chosen as the best one capturing all sources in the area (Supplementary Figure 6). An a-value sensitivity test was done to determine the best range of a-values for each of the four constrained factors: 0.3 (stainless-steel); 0 (nickel refinery); 0 (traffic); 0.3 (solid fuel combustion - SFC); 0.6 (dust). The base run was then calculated from the 8-factor solution with 500 repeats constraining for 5 factors with an exact a-value as calculated by the a-sensitivity test. Runs were selected based on the correlation between the traffic factor and the BC_{ff} and the correlation between SFC and BC_{wb}. The marine factor was then chosen as the one with the largest proportion of Cl; and the S-rich factor as the one with the largest proportion of S. Steelmaking was the profile with the largest Fe proportion. A total of 256 runs (51.2%) were chosen with none missing time points.

The statistical uncertainty of the PMF solution was explored using a bootstrap (BS) resampling strategy. It is a resampling technique of the species concentration and the error matrices where multiple PMF solutions are generated by using a series of data sets resampled from the original input matrix with the same dimensions (number of samples and species) as the original input matrix. Here, one thousand resampled matrices were generated by randomly selecting non-overlapping blocks of 1 day of consecutive samples. PMF was then run on the resampled data. Factors were constrained using the same a-values as in the base run. The same criteria were used to select the unconstrained factors (S-rich, marine and steelmaking). The standard deviation from all BS mapped factor runs was plotted against their mean and the linear fit (reduced-major axis) calculated. The uncertainty of each factor was then calculated as the value of the slope, expressed in percentage (Canonaco, 2019).

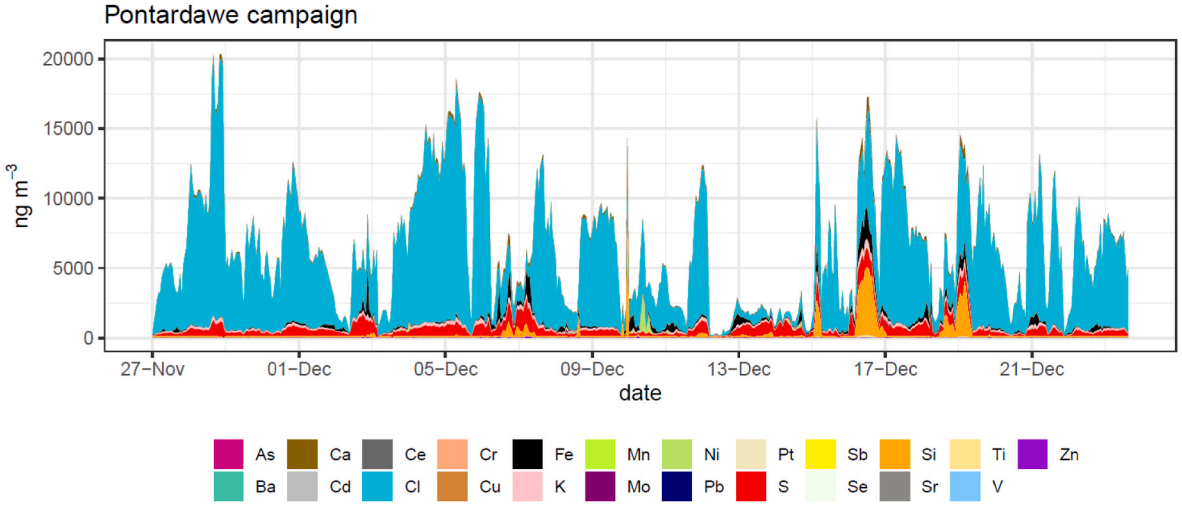

Fig. 2. Time series of the concentrations of the elements measured by the XACT in the Pontardawe campaign.

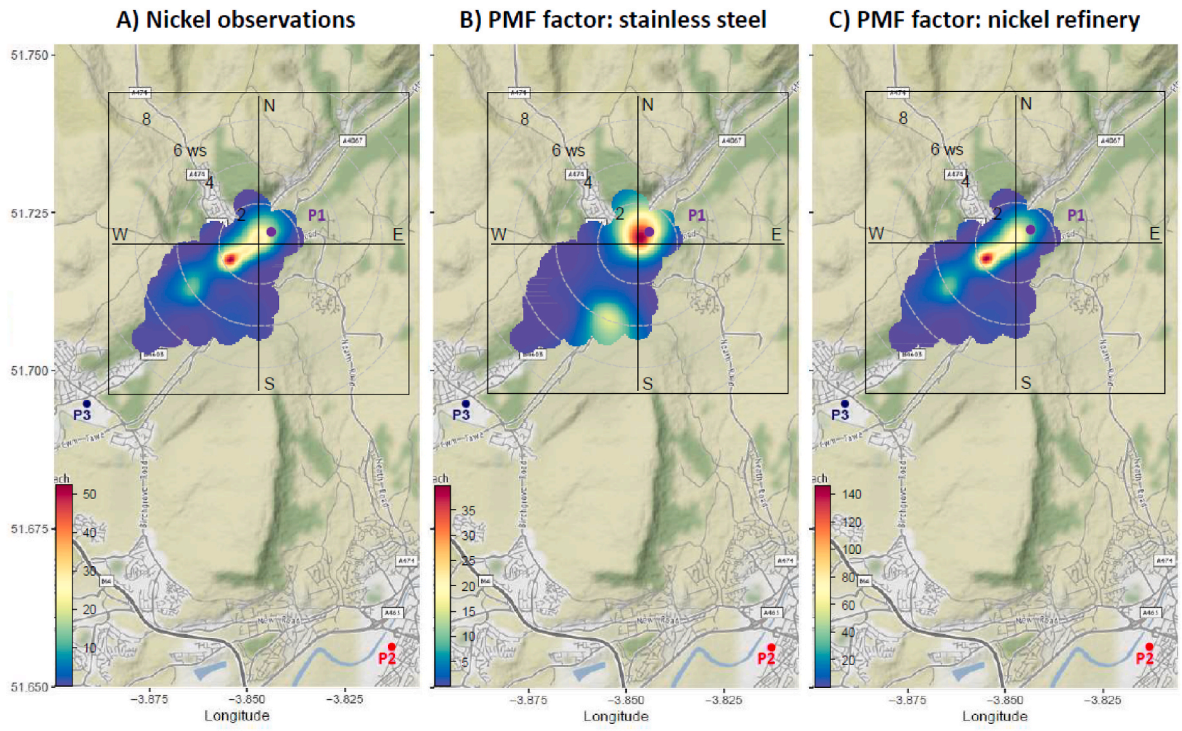

Fig. 3. Mean Bivariate Polar Plot for A) nickel concentrations measured at Pontardawe Tawe Terrace; B) stainless-steel factor from PMF modelling; and C) nickel refinery from PMF modelling. Colour scale: concentrations in ng m^{-3}. Wind speed expressed in m s^{-1}. (For interpretation of the references to colour in this figure legend, the reader is referred to the Web version of this article.)

2.4. Directional analysis

As two industries (P1 and P2) were associated with the production of stainless-steel, directional analysis was undertaken to quantify the contribution of each to the factor concentrations. Bivariate Polar Plots (BPPs) show the mean concentration measured at a site against wind direction and wind speed (Carslaw and Ropkins, 2011) and might be indicative of the position of the main source affecting ambient or modelled concentrations. The *k*-means cluster algorithm applied to a BPP group areas in the plot that have similar features in terms of wind conditions and concentrations. One of the main purposes of clustering on BPP is to identify records in the original time series data by cluster to enable post-processing to better understand potential source characteristics in the time series and characterize potential sources (Carslaw, 2015; Carslaw and Beevers, 2013).

The *k*-means algorithm is detailed in Carslaw and Beevers (2013). Briefly, *k* points are randomly chosen from the data space represented in the original BPPs, which represents the initial group centroids. Each data point of the BPP is therefore assigned to the group based on the closest centroid point and then the position of the *k* centroids recalculated. The two steps are repeated until the centroids no longer move. In this study, the number of optimal clusters in the BPP was evaluated by first computing the *k*-means algorithm from 2 to 9 clusters; and based on the local knowledge of the area (i.e., location of the different industries, topography of the area) the number of optimal clusters was then selected.

3. Results and discussions

3.1. Ambient concentrations

The highest campaign average hourly concentration was for Cl with 5090 ng m^{-3} (Table 1). Sulphur was the second highest in concentration (517 ng m^{-3}). Si (270 ng m^{-3}), Fe (218 ng m^{-3}), Ca (185 ng m^{-3}) and K (151 ng m^{-3}) followed in order of mean concentrations. Ni had a mean concentration of 19.5 ng m^{-3}. The concentrations of Zn, Cr, Mn and Ti in PTT were <10 ng m^{-3}. Time series of element concentrations were dominated by Cl almost all along the campaign with some periods with high Si concentration. S and Fe were also present in all hourly measurements (Fig. 2).

The annual mean concentration of Ni in PM_{10} during 2015 as measured by the weekly samples was 27.8 ng m^{-3} (Goddard et al., 2016). The duration of the current campaign did not allow calculation of the annual mean; however, the mean Ni concentration measured at PTT during the campaign in November–December 2015 was just below the 20 ng m^{-3} threshold. Of note however, PM_{10} Ni concentrations exhibited large variability during the campaign: 0–2480 ng m^{-3} (min – max hourly means), with an inter-quantile range of 2.9 ng m^{-3} (Table 1). The large range in concentrations is an indication of the nature of emissions associated with transient plumes with the most noticeable one measured the first hours on 10 December (Fig. 2). Measured concentrations were also dependent on the wind direction, channelled along the valley according to the location of the main industrial sources (Fig. 3A). The highest concentrations were measured during south-westerly winds (mean hourly Ni concentrations ~50 ng m^{-3}); but also at low wind speeds associated with low dispersion conditions of local sources (mean Ni concentrations ~30 – 40 ng m^{-3}) (Fig. 3A). Ni did not show good temporal correlation to any of the other measured elements at PPT (Supplementary Figure 2).

For the rest of the EU regulated heavy metals (As, Cd and Pb) the mean concentrations measured during the campaign were below the annual mean PM_{10} target limit values: 6, 5 and 500 ng m^{-3} for As, Cd and Pb, respectively.

3.2. PMF

An eight-factor solution was chosen as optimal for the PMF model for the sampling area. The model reproduced 99.1% of the original variability; and the modelled total sum of species showed a slope close to 1, ranging from 0.980 to 1.001 as 95% confidence interval. Only the dust

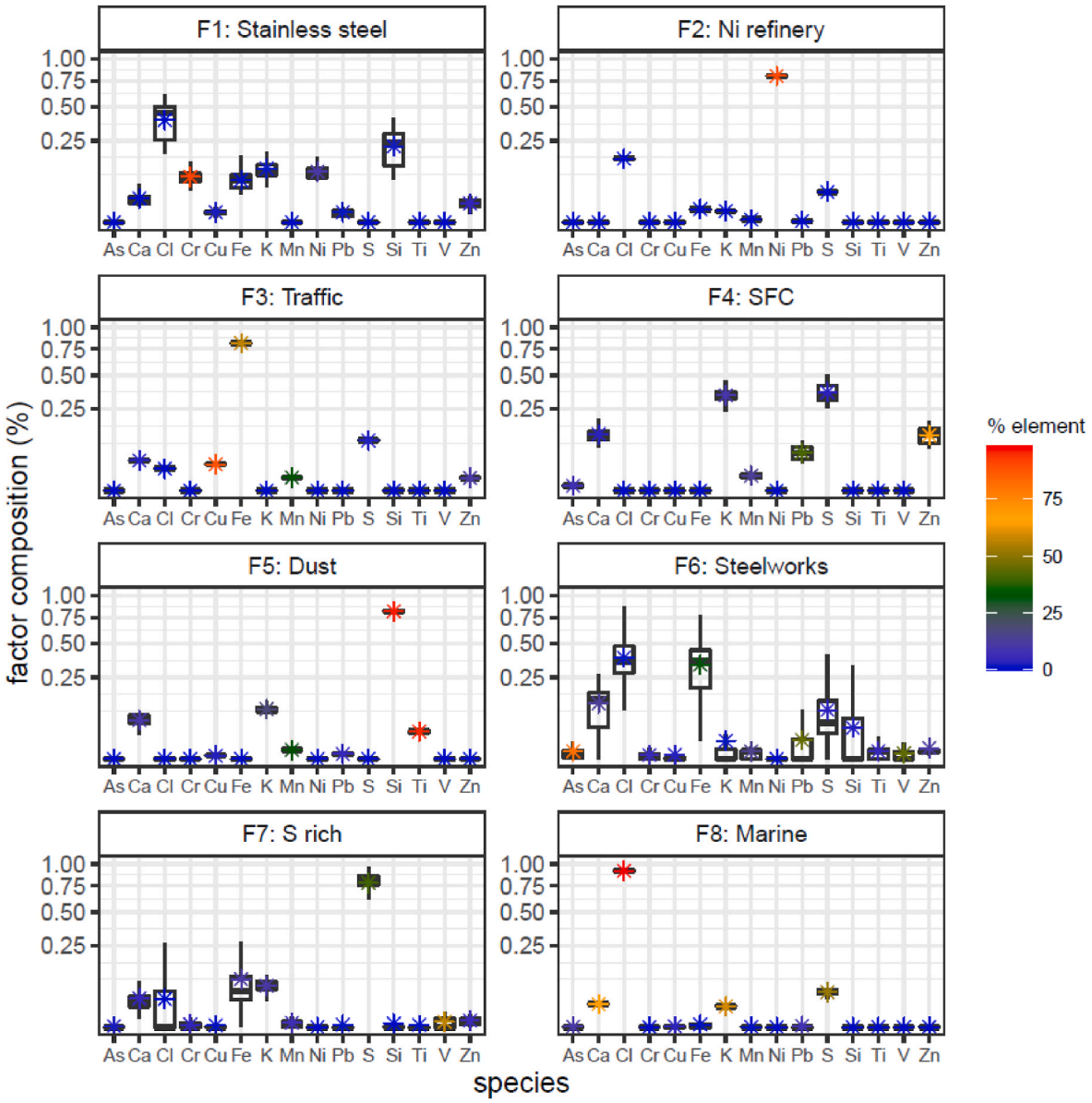

Fig. 4. Chemical composition of each factor at Pontardawe Tawe Terrace. Stars indicate the mean composition for the base run and the colour scale indicate the relative contribution for each element. Boxplots indicate the spread calculated from the BS runs. (For interpretation of the references to colour in this figure legend, the reader is referred to the Web version of this article.)

and the steelmaking factor (F5 and F8) showed a good correlation value (R = 0.85) (Supplementary Figure 6) but very distinct chemical composition (Fig. 4). The scaled residuals for most species showed values between −3 and 3 (Supplementary Figure 7). The statistical uncertainty for each factor ranged between 1% and 53% (Supplementary Figure 8; Supplementary Table 1). The model reproduced well the Ni concentrations, with a slight overestimation of 2%, with a slope close to 1 and an intercept of 0 (Supplementary Figure 9).

The chemical composition for each of the eight factors is shown in Fig. 4; a description of each factor is below.

Factor 1: Stainless-steel. This factor is characterized by the presence of Cr and Ni. The factor also contains Si and Ca, elements used in the stainless-steel production. The bivariate polar plot for this factor showed two source areas, one north and the other south of the monitoring site (Fig. 5) in accordance with the location of P1 and P2, respectively. The random error associated with this factor was 26%.

Factor 2: Nickel refinery. This factor is characterized by the large proportion of Ni (>75% of the factor mass); and also Cl (15% of the profile mass), probably from marine emissions and is consistent with the sea to the south-west (SW). Almost 90% of the Ni measured in the campaign was associated with this factor. The bivariate polar plots for this factor show that the highest contribution took place SW the monitoring site (Fig. 5), according with the position of P3 (Fig. 1). The error associated with this factor was 2%.

Factor 3: Traffic. This factor is characterized by a large fraction of Fe (81%) with tracers of Ca (3%) and Cu (2.5%). Almost 90% of the total Cu measured in the campaign was associated with this factor. Despite Cu being emitted by industrial sources, it is also a tracer of non-exhaust vehicular emissions (Amato et al., 2009). The mean hourly variation of this factor showed two peaks, one at 8–9 am and the second between 4 and 7 pm coinciding with traffic rush hours (Supplementary Figure 10C).

Factor 4: Solid Fuel Combustion. This factor is characterized by a large presence of K on its composition (~40%), with a large presence of S (36%), Ca (12%) and Zn (11%). Pb was also present at a minor proportion (5%). K, Pb and Zn have been associated with wood burning (e.

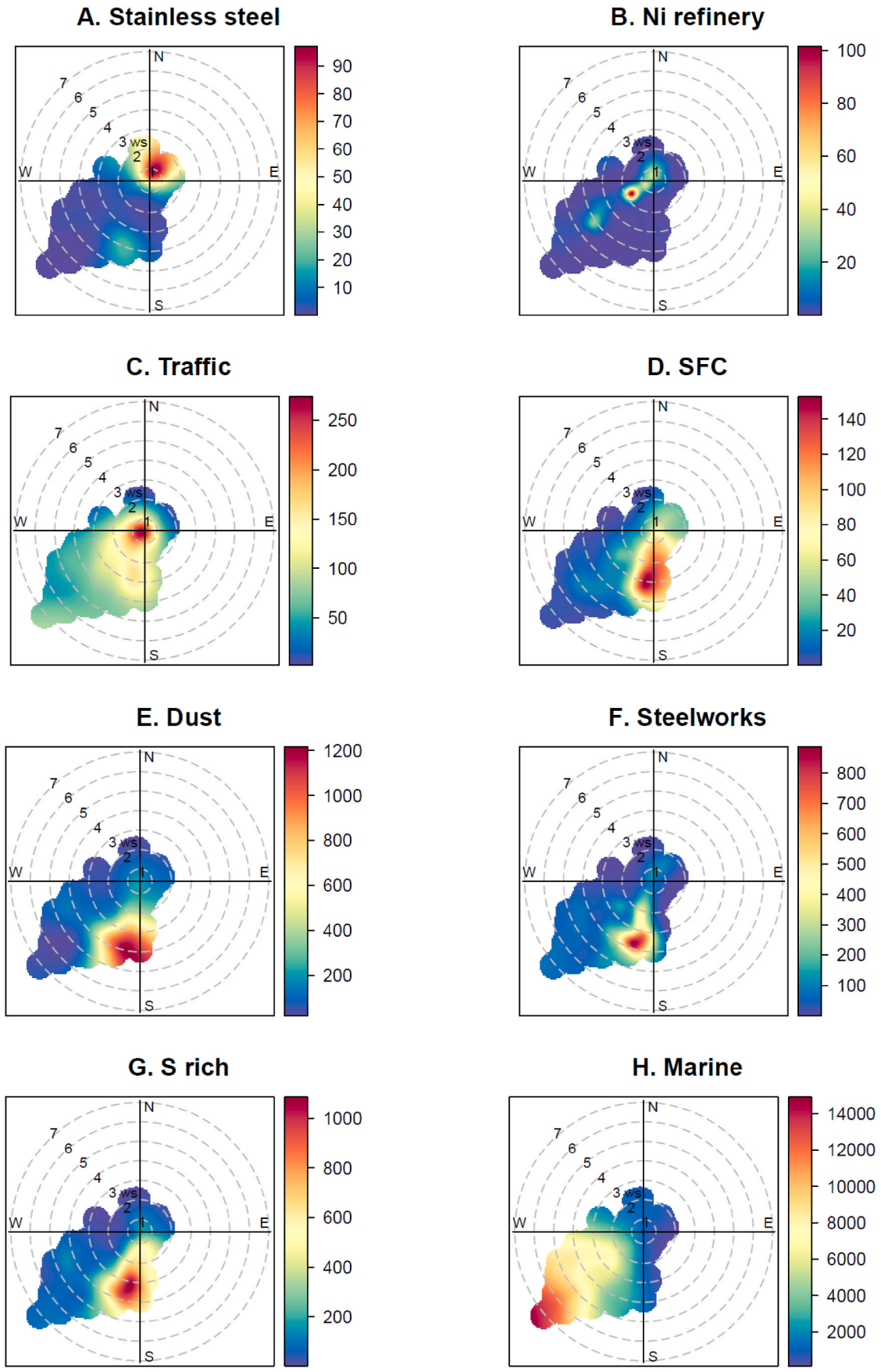

Fig. 5. Bivariate polar plots for each of the sources identified by the base run by the PMF-ME2 at Pontardawe Tawe Terrace.

Table 2
Contribution to the PMF factor and to the Ni concentrations measured at Pontardawe for the different source areas. P1, P2 and P3 refer to the industrial sources showed in Fig. 1.

Source	Mean Ni (ng m^{-3})	Cluster #	Sector (industry)	Contribution to factor (%)	Contribution to Ni (%)
Stainless-steel	2.00	1 + 3	SW	21.5	2.1
		2	S (P3)	12.5	1.2
		5	N (P1)	49.9	6.6
Nickel refinery	18.1		P2		90.1

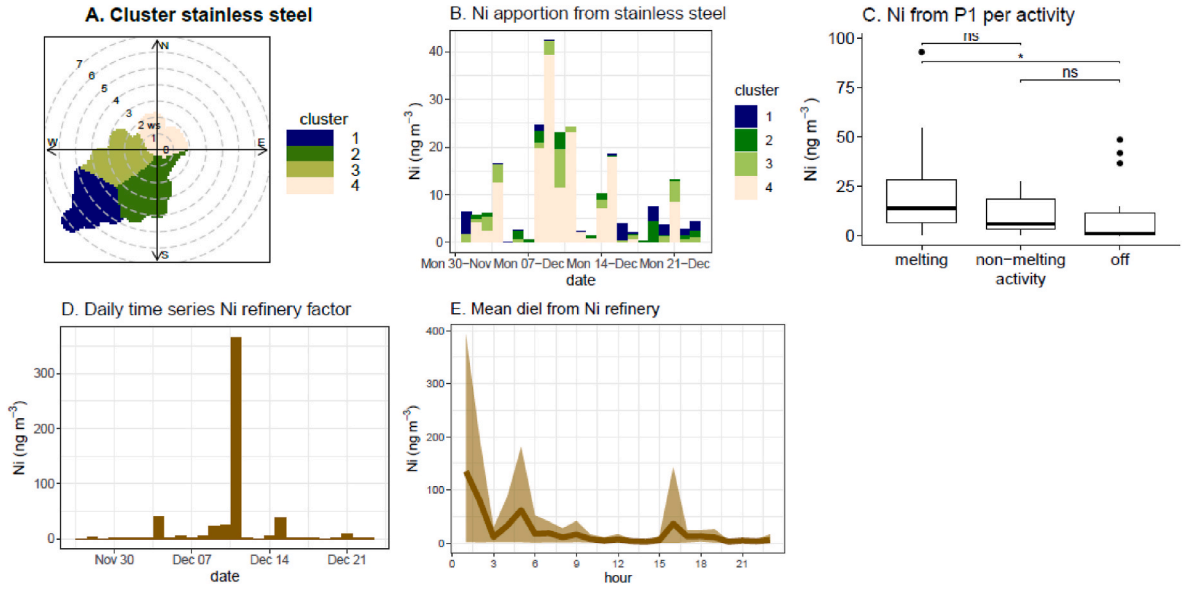

Fig. 6. A. Bivariate Polar Plot (BPP) k-means cluster analysis applied to the timeseries for the stainless-steel factor. B. Daily concentrations of Ni from the stainless-steel factor by cluster. C. Distribution of Ni concentrations modelled from P1 per activity. * statistically significant at level $p < 0.05$; ns = not statistically significant. D. Daily time series of Ni concentrations from the Ni refinery; E. Mean diel plot for Ni from the Ni refinery plot.

g. Maenhaut et al. (2016); Molnár and Sallsten (2013); Watson et al. (2008)).

Factor 5: Dust and Saharan dust. This factor was characterised by mineral tracers such as Si (>80%), K (9%), Ca (6%) and Ti (3%). Almost all Ti measured in the campaign was associated with the Dust factor. The highest contribution from this factor took place on the 17 and December 19, 2015 (Supplementary Figure 11) when an intrusion of Saharan dust occurred in southern England as confirmed by the Hysplit backtrajectory model (Stein et al., 2015) (Supplementary Figure 12).

Factor 6: Steelworks. This profile was characterized by a large proportion of Fe (33%), Ca (11%), S (9%). About 80% of the As measured in the campaign was associated with this profile, 44% for Pb. The polar plot for this factor (Fig. 5) indicates that the sources is located south of the monitoring site, where a steelwork plant is located 20 km away. Fe is associated with the blast furnaces and Ca with sintering processes (Taiwo et al., 2014).

Factor 7 Sulphur rich. This factor is characterized by high proportion of S (>75% of this factor's mass with more than 50% of the total S associated with this factor). The bivariate polar plot for this factor showed a large contribution of the source south of the monitoring site in accordance with the location of the steel plant. Sulphur is associated with coking in the steel making process (Taiwo et al., 2014).

Factor 8: Marine aerosols. It is characterized by a high concentration of chloride (98% of the mass of this factor is composed by Cl) alongside with Ca, K and S (less than 5%). The composition is consistent with sea salt PM generated from the sea with salts such as sodium, chloride, magnesium, calcium, potassium, and sulphate (Querol et al., 2019). The source was measured under SW conditions at high wind speeds (Fig. 5).

3.3. Ni apportionment

Ni was mainly split in two factors: the "nickel refinery" factor and "stainless-steel". The mean concentration of Ni from the Ni refinery factor was 18.1 ng m^{-3} which represented ~90% of the modelled Ni concentrations. The mean Ni concentration from the stainless-steel factor was 2.0 ng m^{-3} which represented slightly ~10% of the modelled Ni (Table 2).

The *k*-means cluster analysis applied to the BPP of the stainless-steel factor returned four areas as the best solution to capture the different source areas for the factor according to the location of industries (Fig. 6A; Supplementary Figure 13). P1 was located north of the monitoring site, in the area within cluster #4 which was the greatest contributor to the factor (~50%), contributing 6.6% to the total Ni burden (Table 2). Contributions from P1 took place mainly during working days (Monday to Friday) (Fig. 6B) when the plant was operating. Mean Ni concentration for activity periods were not statistically different between melting and non-melting hours (Wilcoxon test, $p < 0.05$) but melting hours showed higher Ni concentrations compared to when the plant was not operating (Fig. 6C). Melting hours contributed 66% to the Ni concentrations from P1, 22% was associated with non-activity and possibly due to the resuspension of material. The low contribution from non-melting activities might be related to the low number of available hours (8 h in total) compared to melting activities (25 h) and off hours (17 h). Cluster #2, where emissions from P2 might be contributing, was responsible for ~12% to the stainless-steel factor

and only 1.2% to the Ni burden (Table 2).

The largest contribution from the Ni refinery factor was measured on Friday 11 November, with a mean daily Ni concentration of more than 350 ng m^{-3} (Fig. 6D). The source did not show a clear diel pattern indicating that emissions might be of sporadic nature (Fig. 6E).

4. Conclusions

The measurement station at Pontardawe Tawe Terrace (UK) has been observed to repeatedly exceed the annual EU Target Value for Ni in PM_{10}; most likely due to the local industrial processes. However, which process was most important was unclear from examining the seven-day samples. A 4-week sampling campaign measuring 23 elements in PM_{10} at an hourly time resolution alongside meteorological variables and black carbon was undertaken to provide the highly time resolved data for improved source apportionment. PM_{10} Ni concentrations exhibited a large variability in the hourly concentrations (0–2480 ng m^{-3}) and the campaign mean concentration (19.5 ng m^{-3}) was close to the 20 ng m^{-3} EU target value Ni PM_{10} concentrations were strongly influenced by wind direction and wind speed as this governed both the dispersion of local Ni emissions and the transport from more distant sources. These source characteristics were well represented using bivariate polar plots of Ni, however, this alone was not adequate in distinguishing the different sources, especially between those producing stainless-steel. Multivariate statistical analysis using PMF combined with *k*-means cluster analysis showed that the majority of the Ni PM_{10} concentrations (>90%) were attributed to the nickel refinery. Stainless-steel production from other industrial processes contributed the remaining 10% to the Ni burden, with Ni and Cr as key trace elements.

The application of the *k*-means cluster analysis of the PMF results for the stainless-steel factor improved the identification and quantification of the sources and emitters contributing to the Ni burden. P1 contributed about 7% to the total Ni emissions, with melting activities the greatest contributors. Resuspension of material could be an important source of Ni concentrations from this industrial premises as when it was not operating a contribution of 22% was calculated and therefore associated with resuspension. This apportions of Ni emissions potentially provides and important input into the development of abatement approaches by the industries.

It is unclear how representative measurements collected in November–December 2015 were from the annual mean concentration. Extrapolating the results of the measurement campaign to assess the long-term emissions characteristics of the surrounding industrial processes is challenging. The emissions are transient in nature and meteorological conditions influence the transport and grounding of these emissions. Additional high time resolution measurements would be necessary to understand a wider range of atmospheric conditions at Tawe Terrace on annual basis. Supplementary Figure 1 shows the wind roses from Swansea meteorological station for the whole of 2015 and for Tawe Terrace for the campaign only. It is clear that during the campaign winds were predominantly from the south west. Fewer northerly winds (330°–60°) were observed during the campaign in Nov–Dec 2015 (9.8%) compared to the annual distribution of winds (25.6%). Therefore, the influence from P1 during the campaign was expected to be lower compared to the annual contribution.

This study demonstrates the importance of highly time resolved measurements of conserved tracers of industrial processes, such as metals, to quantify their contribution to atmospheric pollution, especially where the impact of the emission is transient. Non-uniform emission rates and the dependence on meteorological conditions, especially for plume grounding, make the identification and quantification of these sources using poorly time resolved data (e.g. daily) challenging especially where multiple sources are present and despite them making a large contribution to the mean concentrations.

Declaration of competing interest

The authors declare that they have no known competing financial interests or personal relationships that could have appeared to influence the work reported in this paper.

Acknowledgments

The authors would like to thank Martin Hooper at Neath-Port Talbot Council for his help during the organization and deployment of the measurement campaign at Pontardawe; and Simon Baldwin from the Welsh Government for his contribution to the discussion of the results. This study has been partly funded by the Welsh Government under contract C224/2015/2016. It used equipment funded by the Natural Environment Research Council Traffic Grant (NE/1007806/1). The authors gratefully acknowledge the NOAA Air Resources Laboratory (ARL) for the provision of the HYSPLIT transport and dispersion model and READY website (http://www.ready.noaa.gov) used in this publication.

Appendix A. Supplementary data

Supplementary data to this article can be found online at https://doi.org/10.1016/j.envpol.2021.118432.

Authors statement

Anna Font: Conceptualization, Data curation, Formal analysis, Investigation, Methodology, Visualization, Writing - original draft, Anja H. Tremper: Data curation, Investigation, Methodology, Validation, Writing - review and editing, Max Priestman: Data curation, Investigation, Resources, Frank J. Kelly: Funding acquisition, Investigation, Resources, Writing - review and editing, Francesco Canonaco: Conceptualization, Software, Validation, Writing - review and editing, André S. H. Prêvot: Conceptualization, Investigation, Methodology, Validation, Writing - review and editing, David C. Green: Conceptualization, Data curation, Formal analysis, Funding acquisition, Investigation, Methodology, Project administration, Resources, Supervision, Validation, Writing - review and editing.

References

Alastuey, A., Querol, X., Aas, W., Lucarelli, F., Pérez, N., Moreno, T., Cavalli, F., Areskoug, H., Balan, V., Catrambone, M., Ceburnis, D., Cerro, J.C., Conil, S., Gevorgyan, L., Hueglin, C., Imre, K., Jaffrezo, J.L., Leeson, S.R., Mihalopoulos, N., Mitosinkova, M., O'Dowd, C.D., Pey, J., Putaud, J.P., Riffault, V., Ripoll, A., Sciare, J., Sellegri, K., Spindler, G., Espen Yttri, K., 2016. Geochemistry of PM10 over Europe during the EMEP intensive measurement periods in summer 2012 and winter 2013. Atmos. Chem. Phys. 16, 6107–6129. https://doi.org/10.5194/acp-16-6107-2016.

Alleman, L.Y., Lamaison, L., Perdrix, E., Robache, A., Galloo, J.C., 2010. PM10 metal concentrations and source identification using positive matrix factorization and wind sectoring in a French industrial zone. Atmos. Res. 96, 612–625. https://doi.org/10.1016/j.atmosres.2010.02.008.

Amato, F., Pandolfi, M., Escrig, a., Querol, X., Alastuey, a., Pey, J., Perez, N., Hopke, P.K., 2009. Quantifying road dust resuspension in urban environment by Multilinear Engine: a comparison with PMF2. Atmos. Environ. 43, 2770–2780. https://doi.org/10.1016/j.atmosenv.2009.02.039.

Bell, M.L., Belanger, K., Ebisu, K., Gent, J.F., Lee, H.J., Koutrakis, P., Leaderer, B.P., 2010. Prenatal exposure to fine particulate matter and birth weight: variations by particulate constituents and sources. Epidemiology 21, 884–891. https://doi.org/10.1097/EDE.0b013e3181f2f405.

Bell, M.L., Ebisu, K., Leaderer, B.P., Gent, J.F., Lee, H.J., Koutrakis, P., Wang, Y., Dominici, F., Peng, R.D., 2014. Associations of PM2.5 constituents and sources with hospital admissions: analysis of four counties in Connecticut and Massachusetts (USA) for persons ≥ 65 years of age. Environ. Health Perspect. 122, 138–144. https://doi.org/10.1289/ehp.1306656.

Bozlaker, A., Buzcu-Güven, B., Fraser, M.P., Chellam, S., 2013. Insights into PM10sources in Houston, Texas: role of petroleum refineries in enriching lanthanoid metals during episodic emission events. Atmos. Environ. 69, 109–117. https://doi.org/10.1016/j.atmosenv.2012.11.068.

Brown, S.G., Eberly, S., Paatero, P., Norris, G.A., 2015. Methods for estimating uncertainty in PMF solutions: examples with ambient air and water quality data and

guidance on reporting PMF results. Sci. Total Environ. 518–519, 626–635. https://doi.org/10.1016/j.scitotenv.2015.01.022.
Canonaco, F., 2019. Source Finder (SoFi) Manual for the Software Package SoFi and SoFi Pro. IGOR Wavemetrics Inc.
Canonaco, F., Crippa, M., Slowik, J.G., Baltensperger, U., Prévôt, A.S.H., 2013. SoFi, an IGOR-based interface for the efficient use of the generalized multilinear engine (ME-2) for the source apportionment: ME-2 application to aerosol mass spectrometer data. Atmos. Meas. Tech. 6, 3649–3661. https://doi.org/10.5194/amt-6-3649-2013.
Carslaw, D., 2015. The Openair Manual Open-Source Tools for Analysing Air Pollution Data. King's Coll. London, p. 287.
Carslaw, D.C., Beevers, S.D., 2013. Characterising and understanding emission sources using bivariate polar plots and k-means clustering. Environ. Model. Software 40, 325–329. https://doi.org/10.1016/j.envsoft.2012.09.005.
Carslaw, D.C., Ropkins, K., 2011. Open-source Tools for Analysing Air Pollution Data.
Cempel, M., Nikel, G., 2006. Nickel: a review of its sources and environmental toxicology. Pol. J. Environ. Stud. 15, 375–382. https://doi.org/10.1109/TUFFC.2008.827.
Cesari, D., Genga, A., Ielpo, P., Siciliano, M., Mascolo, G., Grasso, F.M., Contini, D., 2014. Source apportionment of PM2.5in the harbour-industrial area of Brindisi (Italy): identification and estimation of the contribution of in-port ship emissions. Sci. Total Environ. 497–498, 392–400. https://doi.org/10.1016/j.scitotenv.2014.08.007.
E-PRTR, 2017. E-PRTR [WWW Document]. Eur. Pollut. Release Transf. Regist. URL. http://prtr.ec.europa.eu.
European Parliament, Council of the European Union, 2004. Directive 2004/107/EC of the European Parliament and of the Council of 15/12/2004 Relating to Arsenic, Cadmium, Mercury, Nickel and Polycyclic Aromatic Hydrocarbons in Ambient Air, pp. 3–17.
Font, A., de Hoogh, K., Leal-Sanchez, M., Ashworth, D.C., Brown, R.J.C., Hansell, A.L., Fuller, G.W., 2015. Using metal ratios to detect emissions from municipal waste incinerators in ambient air pollution data. Atmos. Environ. 113 https://doi.org/10.1016/j.atmosenv.2015.05.002.
Fuller, G.W., Tremper, A.H., Baker, T.D., Yttri, K.E., Butterfield, D., 2014. Contribution of wood burning to PM10 in London. Atmos. Environ. 87, 87–94. https://doi.org/10.1016/j.atmosenv.2013.12.037.
Furger, M., Minguillón, M.C., Yadav, V., Slowik, J.G., Hüglin, C., Fröhlich, R., Petterson, K., Baltensperger, U., Prévôt, A.S.H., 2017. Elemental composition of ambient aerosols measured with high temporal resolution using an online XRF spectrometer. Atmos. Meas. Tech. 10, 2061–2076. https://doi.org/10.5194/amt-10-2061-2017.
Goddard, S.L., Brown, R.J.C., Butterfield, D., McGhee, E.A., Robins, C., Brown, A., Beccaceci, S., Lilley, A., Bradshaw, C., Brennan, S., 2015. Annual Report for 2014 on the UK Heavy Metals Monitoring Network.
Goddard, S.L., Brown, R.J.C., Robins, C., Lilley, A., 2016. Annual Report for 2015 on the UK Heavy Metals Monitoring Network.
Kara, M., Hopke, P.K., Dumanoglu, Y., Altiok, H., Elbir, T., Odabasi, M., Bayram, A., 2015. Characterization of PM using multiple site data in a heavily industrialized region of Turkey. Aerosol Air Qual. Res. 15, 11–27. https://doi.org/10.4209/aaqr.2014.02.0039.
Kfoury, A., Ledoux, F., Roche, C., Delmaire, G., Roussel, G., Courcot, D., 2016. PM2.5source apportionment in a French urban coastal site under steelworks emission influences using constrained non-negative matrix factorization receptor model. J. Environ. Sci. (China) 40, 114–128. https://doi.org/10.1016/j.jes.2015.10.025.
MacIejczyk, P., Zhong, M., Lippmann, M., Chen, L.C., 2010. Oxidant generation capacity of source-apportioned PM2.5. Inhal. Toxicol. 22, 29–36. https://doi.org/10.3109/08958378.2010.509368.
Maenhaut, W., Vermeylen, R., Claeys, M., Vercauteren, J., Roekens, E., 2016. Sources of the PM10 aerosol in Flanders, Belgium, and re-assessment of the contribution from wood burning. Sci. Total Environ. 562, 550–560. https://doi.org/10.1016/j.scitotenv.2016.04.074.
Martin, P., Parton, T., Pyatt, R., Bennett, A., Price, A., 2019. Industrial Fuel Switching-Project ASPIRE. Gov.uk, pp. 1–42.
Molnár, P., Sallsten, G., 2013. Contribution to PM2.5 from domestic wood burning in a small community in Sweden. Environ. Sci. Process. Impacts 15, 833–838. https://doi.org/10.1039/c3em30864b.
Mooibroek, D., Schaap, M., Weijers, E.P., Hoogerbrugge, R., 2011. Source apportionment and spatial variability of PM 2 . 5 using measurements at fi ve sites in The Netherlands. Atmos. Environ. 45, 4180–4191. https://doi.org/10.1016/j.atmosenv.2011.05.017.
Nriagu, J.O., Pacyna, J.M., 1988. Quantitative assessment of worldwide contamination of air, water and soils by trace metals. Nature 333, 134–139. https://doi.org/10.1038/333134a0.
Paatero, P., 1999. The multilinear engine—a table-driven, least squares program for solving multilinear problems, including the n-way parallel factor Analysis model. J. Comput. Graph Stat. 8, 854–888. https://doi.org/10.1080/10618600.1999.10474853.
Paatero, P., Hopke, P.K., 2003. Discarding or downweighting high-noise variables in factor analytic models. Anal. Chim. Acta 490, 277–289. https://doi.org/10.1016/S0003-2670(02)01643-4.
Paatero, P., Tapper, U., 1994. Positive matrix factorization: a non-negative factor model with optimal utilization of error estimates of data values. Environmetrics 5, 111–126. https://doi.org/10.1002/env.3170050203.
Pacyna, J.M., Semb, A., Hanssen, J.E., Pacyna, B.J.M., Semb, A., Hanssen, J.A.N.E., 1984. Tellus B : chemical and Physical Meteorology Emission and long-range transport of trace elements in Europe Emission and long-range transport of trace elements in Europe 36. https://doi.org/10.3402/tellusb.v36i3.14886, 3, 163, 178.
Pandolfi, M., Gonzalez-Castanedo, Y., Alastuey, A., de la Rosa, J.D., Mantilla, E., de la Campa, A.S., Querol, X., Pey, J., Amato, F., Moreno, T., 2011. Source apportionment of PM10 and PM2.5 at multiple sites in the strait of Gibraltar by PMF: impact of shipping emissions. Environ. Sci. Pollut. Res. 18, 260–269. https://doi.org/10.1007/s11356-010-0373-4.
Peltier, R.E., Hsu, S.I., Lall, R., Lippmann, M., 2009. Residual oil combustion: a major source of airborne nickel in New York City. J. Expo. Sci. Environ. Epidemiol. 19, 603–612. https://doi.org/10.1038/jes.2008.60.
Querol, X., Tobías, A., Pérez, N., Karanasiou, A., Amato, F., Stafoggia, M., Pérez García-Pando, C., Ginoux, P., Forastiere, F., Gumy, S., Mudu, P., Alastuey, A., 2019. Monitoring the impact of desert dust outbreaks for air quality for health studies. Environ. Int. 130, 104867. https://doi.org/10.1016/j.envint.2019.05.061.
Querol, X., Viana, M., Alastuey, A., Amato, F., Moreno, T., Castillo, S., Pey, J., de la Rosa, J., Sánchez de la Campa, A., Artíñano, B., Salvador, P., García Dos Santos, S., Fernández-Patier, R., Moreno-Grau, S., Negral, L., Minguillón, M.C., Monfort, E., Gil, J.I., Inza, A., Ortega, L.A., Santamaría, J.M., Zabalza, J., 2007. Source origin of trace elements in PM from regional background, urban and industrial sites of Spain. Atmos. Environ. 41, 7219–7231. https://doi.org/10.1016/j.atmosenv.2007.05.022.
Rai, P., Furger, M., El Haddad, I., Kumar, V., Wang, L., Singh, A., Dixit, K., Bhattu, D., Petit, J.E., Ganguly, D., Rastogi, N., Baltensperger, U., Tripathi, S.N., Slowik, J.G., Prévôt, A.S.H., 2020. Real-time measurement and source apportionment of elements in Delhi's atmosphere. Sci. Total Environ. 742, 140332. https://doi.org/10.1016/j.scitotenv.2020.140332.
Sánchez de la Campa, A.M., Moreno, T., de la Rosa, J., Alastuey, A., Querol, X., 2011. Size distribution and chemical composition of metalliferous stack emissions in the San Roque petroleum refinery complex, southern Spain. J. Hazard Mater. 190, 713–722. https://doi.org/10.1016/j.jhazmat.2011.03.104.
Sandradewi, J., Prévôt, A.S.H., Szidat, S., Perron, N., Alfarra, M.R., Lanz, V.a., Weingartner, E., Baltensperger, U., 2008. Using aerosol light absorption measurements for the quantitative determination of wood burning and traffic emission contribution to particulate matter. Environ. Sci. Technol. 42, 3316–3323. https://doi.org/10.1021/es702253m.
Stein, A.F., Draxler, R.R., Rolph, G.D., Stunder, B.J.B., Cohen, M.D., Ngan, F., 2015. Noaa's hysplit atmospheric transport and dispersion modeling system. Bull. Am. Meteorol. Soc. https://doi.org/10.1175/BAMS-D-14-00110.1.
Taiwo, A.M., Beddows, D.C.S., Calzolai, G., Harrison, R.M., Lucarelli, F., Nava, S., Shi, Z., Valli, G., Vecchi, R., 2014. Receptor modelling of airborne particulate matter in the vicinity of a major steelworks site. Sci. Total Environ. 490, 488–500. https://doi.org/10.1016/j.scitotenv.2014.04.118.
Tremper, A.H., Font, A., Priestman, M., Hamad, S.H., Chung, T.-C., Pribadi, A.5, Brown, R.J.C., Goddard, S.L., Grassineau, N., Petterson, K., Kelly, F.J., Green, D.C., 2017. Field and laboratory evaluation of a high time resolution x- ray fluorescence instrument for determining the elemental composition of ambient aerosols. Atmos. Meas. Tech. Discuss 5194, 2017–2363. https://doi.org/10.5194/amt-2017-363.
US EPA, 2016. Iron and steel foundries: national emissions standards for hazardous air pollutants (NESHAP) [WWW Document]. United States Environ. Prot. Agency. URL. https://www.epa.gov/stationary-sources-air-pollution/iron-and-steel-foundries-national-emissions-standards-hazardous-air.
Viana, M., Hammingh, P., Colette, A., Querol, X., Degraeuwe, B., Vlieger, I. De, van Aardenne, J., 2014. Impact of maritime transport emissions on coastal air quality in Europe. Atmos. Environ. 90, 96–105. https://doi.org/10.1016/j.atmosenv.2014.03.046.
Virkkula, a., Chi, X., Ding, a., Shen, Y., Nie, W., Qi, X., Zheng, L., Huang, X., Xie, Y., Wang, J., Petäjä, T., Kulmala, M., 2015. On the interpretation of the loading correction of the aethalometer. Atmos. Meas. Tech. Discuss. 8, 7373–7411. https://doi.org/10.5194/amtd-8-7373-2015.
Watson, J.G., Chen, L.W.A., Chow, J.C., Doraiswamy, P., Lowenthal, D.H., 2008. Source apportionment: findings from the U.S. supersites program. J. Air Waste Manag. Assoc. 58, 265–288. https://doi.org/10.3155/1047-3289.58.2.265.
Zhang, Z., Chau, P.Y.K., Lai, H.K., Wong, C.M., 2009. A review of effects of particulate matter-associated nickel and vanadium species on cardiovascular and respiratory systems. Int. J. Environ. Health Res. 19, 175–185. https://doi.org/10.1080/09603120802460392.